

# Pinpointing Why Object Recognition Performance Degrades Across Income Levels and Geographies

Laura Gustafson, Megan Richards, Melissa Hall, Caner Hazirbas, Diane Bouchacourt, Mark Ibrahim

Fundamental AI Research (FAIR), Meta AI

## Abstract

Despite impressive advances in object-recognition, deep learning systems’ performance degrades significantly across geographies and lower income levels—raising pressing concerns of inequity. Addressing such performance gaps remains a challenge, as little is understood about why performance degrades across incomes or geographies. We take a step in this direction by annotating images from Dollar Street, a popular benchmark of geographically and economically diverse images, labeling each image with factors such as color, shape, and background. These annotations unlock a new granular view into how objects differ across incomes/regions. We then use these object differences to pinpoint model vulnerabilities across incomes and regions. We study a range of modern vision models, finding that performance disparities are most associated with differences in *texture*, *occlusion*, and images with *darker lighting*. We illustrate how insights from our factor labels can surface mitigations to improve models’ performance disparities. As an example, we show that mitigating a model’s vulnerability to texture can improve performance on the lower income level. We release all the **factor annotations** along with an **interactive dashboard** to facilitate research into more equitable vision systems.

## 1 Introduction

The widespread adoption of object-recognition systems afforded by advances in deep learning comes with a responsibility: systems should work equally well across groups of individuals. Previous work demonstrates object-recognition performance is far from equal across income levels and geographies [7, 14, 23]. This disparity encompasses publicly available recognition systems, state-of-the-

### Model vulnerabilities explain performance drops

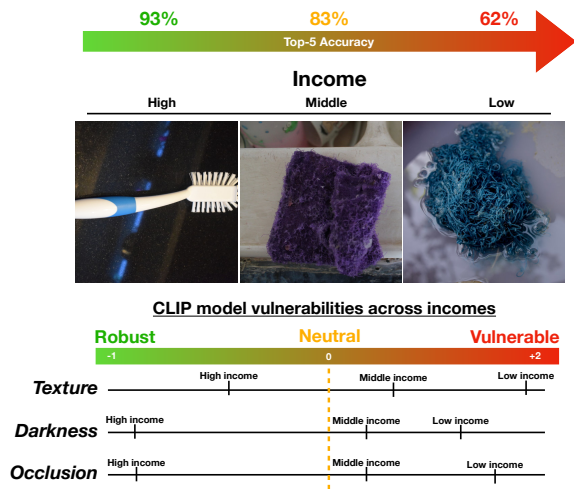


Figure 1: CLIP’s vulnerability to texture, darker lighting, and occlusion are associated with performance disparities for lower incomes. We rank the most vulnerable factors based on how much more likely a factor is selected among misclassified images than overall. The example images are of *dishbrushes* from Dollar Street.

art supervised and self-supervised models. Most worrisome among these findings is that the performance degradation disproportionately affects lower income households. When Artificial Intelligence (AI) systems are deployed in applications such as medical imaging, their biases can lead to disproportional harm. For example, models diagnosing COVID-19 were found to rely on geographically-biased features such as the hospital’s font to diagnose patients [22].

While existing work measures performance disparities across incomes and geographies, addressing the perfor-

mance gaps remains a challenge. Key to progress is understanding *not just that, but why such disparities arise*. One hypothesis raised in De Vries et al. [7] is that objects as well as their environments can vary drastically across regions. When factors such as object shape or lighting in a region differ from those commonly seen during training, the shift can cause model performance to drop. However, no systematic study exists characterizing how such factors vary across regions and incomes. Identifying the factors associated with model disparities can shed light on research directions to improve performance degradation across incomes and geographies.

We take a step in this direction by annotating images from Dollar Street [23], a common benchmark for evaluating performance disparities in object recognition systems. Dollar Street contains 38k images of household objects spanning 54 countries across income levels. We annotate each image with factors to mark what makes each distinctive, such as color, pose, shape, and texture. We first analyze how images vary across incomes and regions using our factor labels in Section 3. We find images of some classes such as *roofs* differ considerably across regions (and incomes) while others (such as *pens*) hardly vary.

We then investigate how our factor labels can explain model mistakes. We find an overall correspondence between the distribution of factors per region (and income) and model performance. Even for the latest generation of foundation models, such as CLIP [19], performance degrades by as much as 25.7% (top-5 accuracy) across incomes. We also compare the performance of other popular models across learning paradigms (self-supervised, supervised), architectures (CNN-, transformer-, MLP-based), as well as large scale pretraining [12]. We find remarkably similar vulnerabilities across these popular models.

Next, we precisely rank factors by examining how much more likely they are to appear among misclassifications. A factor much more likely to appear among misclassification suggests a model is vulnerable to the factor. In our analysis we find vulnerabilities in *texture*, *occlusion*, and *darker lighting* are most associated with models’ performance degradation in lower incomes as illustrated in Figure 1. We further study class-specific model vulnerabilities, finding strong associations between mistakes for particular classes and factors. For example, we find that for *sofas*, images labeled with texture are 7.2x more likely to appear among CLIP’s mistakes than overall, suggesting texture bias is a

vulnerability.

Finally, we study whether we can use robustness techniques to make fairness improvements. We show that mitigating the texture vulnerability surfaced by our analysis can improve performance disparities across incomes/regions in Section 6.2. We find a model trained to mitigate texture bias not only performs better overall +0.8% (top-5 accuracy), but on the relevant subset of images (those marked with `texture`), improves accuracy by 4.1% for `low` incomes. This suggests factor labels not only explain mistakes, but can even reveal promising mitigations to combat the disparities we observe in vision models today. Along with our analysis, we release all the factor annotations with an interactive dashboard to enable research facilitating more responsible, equitable vision system.

To summarize, our contributions are 1) we annotate all of Dollar Street images with distinctive factor labels such as pose, background, and color, 2) we explain performance disparities in models (including CLIP) using our factor annotations to reveal vulnerabilities in texture, occlusion, and darker lighting, 3) we demonstrate mitigating the vulnerability to texture can improve performance disparities across incomes and geographies, 4) we release all our factor annotations with a dashboard (Figure 2) allowing researchers to interactively query and visualize image factor labels to spur research into equitable vision systems.

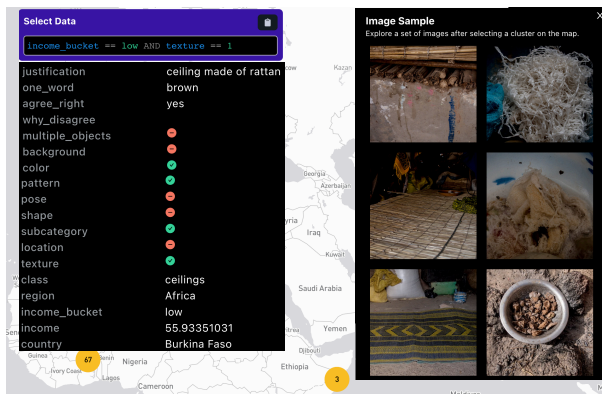


Figure 2: A screenshot of our **interactive dashboard** allowing researchers to query subsets, visualize images, and view our corresponding factor labels.

## 2 Annotating Dollar Street with factor labels

The Dollar Street dataset is a common computer vision benchmark for classifying everyday objects (e.g. *armchairs*, *toothbrush*, *pens*) across incomes and geographies. Households across the world upload images of the specified objects. These images are labeled with the object class, location, and income of the household. The income is standardized on an international scale by DollarStreet [1]. We use the procedure described in [14] to aggregate household incomes into buckets: `high`, `medium` and `low`, and group countries into regions: `Asia`, `Africa`, `Europe`, `The Americas`. Table 4 in Appendix A.1.1 shows the number of images per income bucket/region pair.

### 2.1 Annotation Procedure

In order to explain the degradation in model performance across incomes or geographies, annotators labeled images in Dollar Street with the factors distinguishing each image. We select all 14k images overlapping with classes in the ImageNet-21k taxonomy from Ridnik et al. [21], using the mapping from DollarStreet classes to ImageNet synsets from Goyal et al. [14]. We follow the same annotation procedure as in Idrissi et al. [16]. Since it’s challenging to accurately label an image in isolation, we ask annotators to label how each image differs from a fixed set of three prototypical images chosen for each class. We define prototypical images for each class as those correctly classified by a ResNet-50 model with the highest confidence. We curate a list of sixteen potential factors that can distinguish an image from the prototypical images for its class. These factors include pose, various forms of occlusion, size, style, type or breed. A full list is shown in Figure 3. Annotators select any number of factors they believe best distinguish each image. In addition, we ask annotators to provide text descriptions to account for factors outside the sixteen factors we provide, and ask if they agree with the original class label (see 2.3 for further discussion of how this was used). A more detailed description of the annotation setup and prototypical images is in Appendix A.1.

### 2.2 Factor label statistics

We first explore how frequently each factor was selected across income levels and regions. In Figure 3, we plot

the distribution of factor labels across regions and income buckets. On average, annotators chose 3.2 factors per image (standard deviation 1.2). The two most correlated factors are *color* and *pattern*, with a correlation coefficient of 0.19.

**Across all incomes, *pose*, *background*, and *pattern* are the most selected factors.** For most factors, there is only a minor difference in the frequency that a factor was selected across income buckets. For *texture*, however, there’s a noteworthy difference across income levels with 10.2% of images in the `low` income bucket labeled with *texture* compared to only 4.2% for `medium` and 2.0% for `high` income buckets. This implies *texture* is 5x more likely to be selected within the `low` income bucket (relative to the `high` income bucket), a stark difference.

**The most commonly selected factors are consistent across regions and incomes.** Similar to our observation across income buckets, the most striking difference across regions is for *texture*. *Texture* is selected for 7.8% of images in `Africa` but for only 2% of images in `Europe`—a 4x difference. The similarity of emerging patterns in factors across incomes to those across regions suggests that income bucket variation differences are also exhibited across geographies. This can in part be explained by the relative rates of co-occurrence of regions and income buckets in DollarStreet, see Table 4 in Appendix A.1.1.

### 2.3 Controlling for regional differences in raters’ perceptions

Challenges naturally arise when running such a large annotation procedure. In our case, there can exist regional perceptions of the semantic meaning of every object label. Indeed, the Dollar Street object class labels were originally collected from the household members who took the image, rather than assigned retroactively, which means that regional perceptions could be a source of variance in the dataset. To control for the effect of such perceptual differences across regions, we created a second annotation task. To select the images for the task, we analyzed the results of the original factor annotations, which included an option for annotators to disagree with the object label. We selected the subset of images where the annotator

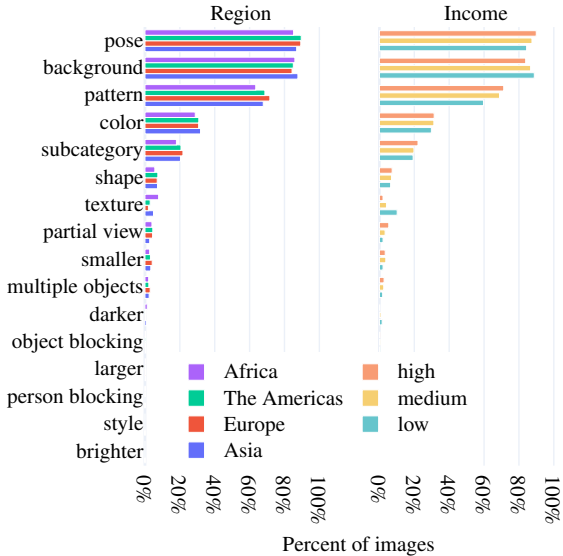


Figure 3: **Pose, background, and pattern are the most commonly selected factors.** Figure shows the percent of images by region and income that were labelled with each factor. Annotators labelled each image with the factors that most distinguished each image from the prototypical images of its class.

disagreed with the label, which totaled 2,476 images, or 18.1% of the Dollar Street dataset. For the second task, we collected additional annotations for this disputed subset, asking annotators sourced from 6 countries (5 continents) whether they agreed or disagreed with the object label. In total, there were 79 annotators who provided 12,507 label annotations. See Appendix A.1.4 for examples of annotator disagreements, and classes with the highest and lowest levels of label disagreement.

We then compared the levels of disagreement between annotators from the region where the image was taken (source region) and annotators who were from other regions. If there were region-specific biases in the label, we would expect a much higher rate of disagreement for annotators not from the source region. For images in the second task, we found annotators from both the source and other regions disagreed with the original label at similar rates (an average of 49.1% and 46.8% respectively). This con-

sistency suggests regional differences in label perceptions do not constitute a significant source of class variation in Dollar Street. As a result, we can turn to our factor annotations to characterize how class images vary across regions and incomes.

### 3 How do objects vary across incomes and geographies?

Leveraging the factors gathered in our annotation process, we can quantitatively assess how classes differ across incomes and regions. For example, we can identify classes that change the most across incomes (e.g. ceiling), as well as the corresponding factors that best differentiated high or low income ceilings (pose, subcategory, and texture).

To compare how classes differ across two regions (or incomes), we compute the distribution of factors for each class. Specifically, for every pair of regions (or incomes) we normalize the distributions per class then measure the Jensen-Shannon Distance (JSD) to characterize how images differ across regions (or incomes). Note the Jensen-Shannon Distance is the square root of Jensen-Shannon divergence between two distributions, and is a standard metric to compare discrete distributions [9]. A large JSD distance between two regions for a class indicates images differ across those regions.

**Some classes’ factors vary significantly across incomes and regions; others remain consistent.** In Table 1, we show the most starkly different classes across incomes/regions, along with their most distinguishing factors. Consistently, we find the largest differences are between low and high incomes, but don’t find a consistent pattern with regions. For classes with the largest differences across regions/incomes, we find these differences to be significant with an average JSD more than twice the median JSD of all classes (across incomes/regions). Among classes differing most across regions are those relating to animals (*chickens, pet foods*); those differing most across incomes relate to building structures (*roofs, ceiling, floors*). We report full tables for the most similar and dissimilar classes across regions and incomes in Appendix A.2. In contrast, other classes don’t vary across incomes/regions such as *vegetable pots, phones, and pens* as shown in Figure 4.

class	income bucket	differentiating factors
<i>Most stark difference by income</i>		
roofs	low vs high	subcategory, pose, smaller
ceilings	low vs high	pose, subcategory, texture
diapers	low vs high	color, shape, texture
radios	low vs high	color, shape, subcategory
floors	low vs high	texture, pose, pattern
<i>Most stark difference by region</i>		
chickens	Asia vs Europe	partial view, color, shape
chickens	Europe vs Africa	pose, partial view, color
diapers	Americas vs Africa	pose, color, partial view
pet foods	Asia vs Americas	color, texture, pattern
pet foods	Asia vs Europe	pattern, subcategory, color

Table 1: Classes with most stark differences in factor distributions by Jensen-Shannon Distance (JSD) across incomes/regions.



Figure 4: Example images for roofs, the class with the largest factor variation across incomes, and vegetable plots, the class with the smallest factor variation across income.

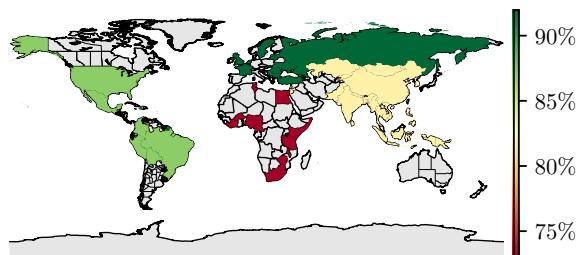
This suggests that while some classes can vary drastically across incomes or regions, others are quite similar.

## 4 Modern models’ performance degrades across incomes and geographies

We first study the popular foundation model CLIP, which has been shown to have strong zero-shot performance on several classification benchmarks [19]. CLIP is trained on 400M text-image pairs using a text encoder and an image encoder enabling a user to perform zero shot classification for any image. Here we prompt the model using the set of Dollar Street classes for each image to generate predictions. Our evaluation setup is described in detail in Appendix A.3.

We show the performance of CLIP ViT B/32 on DollarStreet across income and geographies in Figure 5. Despite impressive performance across several other classification and robustness benchmarks, we find performance drops by 25.7% from high to low incomes. We observe similar drops across regions. Overall the performance disparities for CLIP are comparable to those observed for other models in prior work [14], suggesting performance disparities remain even in the latest generation of foundation models. Next we conduct a more comprehensive analysis of performance disparities across other model types.

**Performance inequities are pervasive across architectures and training methods.** We expand our study to encompass models across architectures (convolutional, transformer, and feedforward), learning paradigms (self-supervised and supervised), and pretraining datasets of various sizes (up to 1 billion images). To generate predictions on Dollar Street, the images are pretrained or finetuned on ImageNet21k and we use the same mapping from Goyal et al. [14] and detail our evaluation procedure in Appendix A.3. We compare the performance of the set of models across incomes and regions in Figures 6 and 7. We find most models have comparable drops in accuracy across incomes and regions despite model differences. BEiT performs worse overall, but still exhibits similar trends in performance gaps across incomes and ge-



Income Bucket	Top 5 Accuracy
Low	66.9
Middle	83.4
High	92.6

Figure 5: **CLIP performance degrades across incomes and geographies.** Shows CLIP ViT B/32 top-5 accuracy per region and income bucket. Color indicates model performance per region.

geographies [2]. This suggests even large scale pretraining in models such as SEER [13], modern architectures such as ViT [21] or MLP Mixer [27], and self-supervised learning still don't address performance inequities. Why do such consistent disparities arise? Next we study whether factors labels can explain the performance disparities in modern vision models.

## 5 Explaining model performance disparities with factor labels

We now study how our factor labels can explain the model performance disparities we observed across regions/incomes. After ruling out variables such as image quality and class imbalance in training, we demonstrate how our factor labels can surface specific model vulnerabilities associated with degradation in performance across regions/incomes.

### 5.1 Controlling for factors not captured in our annotations

**Performance disparities are not explained by image quality or training data class imbalance.** As image

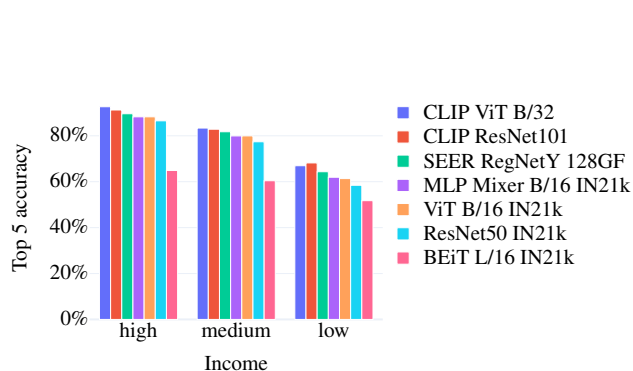


Figure 6: **Across architectures and learning procedures, model performance degrades similarly for lower incomes.** Bars indicate top-5 accuracy.

quality has been shown to impact the performance of facial recognition models [29], we first investigate whether image resolutions differ across regions and effect model performance. Rojas et al. [23] found very minor differences in average image quality across region in DollarStreet. We take this a step further and find no strong correlation ( $< 0.05$  Pearson's correlation coefficient) between image DPI and model performance (top-5 accuracy). Next, since class imbalance in training can skew model performance, we also investigate the extent to which class imbalance affects the disparities we observe. For ImageNet-21K pretrained or finetuned models (ViT, ResNet, MLPmixer, BEiT, and SEER), we calculate the Pearson correlation between number of images in each class for ImageNet-21K and model's top-5 accuracy. We found similarly weak correlations for all models, with coefficients less than 0.25 for top-5 accuracy (all values reported in Appendix A.4). These results suggest that variation in image quality and pretraining class imbalance explain very little of the variation model mistakes in Dollar Street. Next, we examine whether our factor labels can explain model performance disparities.

### 5.2 Variation in factor labels are indicative of performance disparities

To assess whether our factor labels are indicative of model performance disparities, we measure whether larger differ-

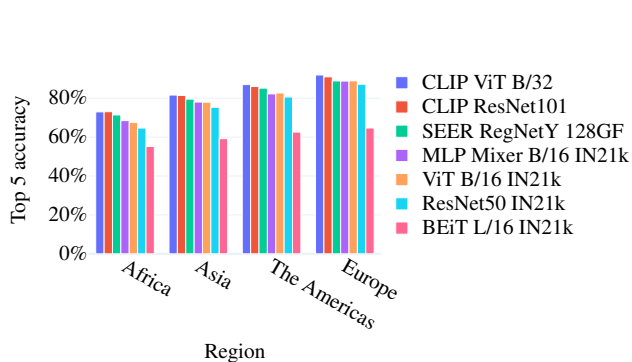


Figure 7: **Across architectures and learning procedures, model performance degrades similarly across geographies.** Bars indicate top-5 accuracy.

ences in factor labels across incomes/regions correspond to larger degradations in model performance. Specifically, for each class we measure the Jensen Shannon Distances (JSD) between the factor label distributions of every pair of income buckets (and regions). This quantifies how images in a classes vary across income bucket (or region) pairs according to our factor labels.

Next, we calculate whether larger differences in images across incomes/regions correspond to larger disparities in model performance. We find as a class varies more across income pairs (according to the JSD of factor distributions), model performance gaps also increase, as shown in Figure 8. For example, classes that differ most across incomes (top quarter) suffer a 3x drop in accuracy compared to classes that differ the least across incomes (bottom quarter). We find a similar but less stark trend across regions shown in Figure 8. These results suggest *our factor labels can explain model performance disparities across regions/incomes.*

### 5.3 Model performance disparities are most associated with texture, darker lighting, and occlusion

To more precisely assess which factors are most associated with mistakes, we use the same error ratio metric from Idrissi et al. [16] to measure the association between each

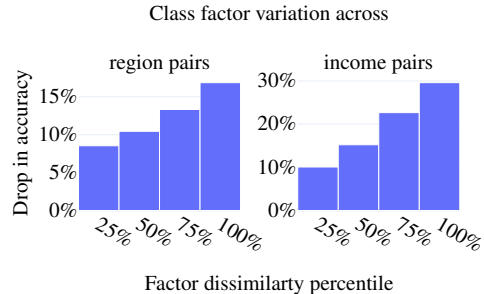


Figure 8: **Differences across regions/incomes measured by our factor labels are indicative of performance disparities.** The factor dissimilarity measures the distance (JSD) in factor label distributions across two regions/incomes for a specific class. The drop in accuracy measures the drop in performance for the given class across two regions/incomes.

factor and model errors. Specifically, the error ratio for a factor quantifies how much more or less likely a factor is to appear among a model’s misclassified samples as

$$\frac{P(\text{factor X} \mid \text{model errors}) - P(\text{factor X})}{P(\text{factor X})} \quad (1)$$

An error ratio greater than zero indicates how much more likely a factor is to appear among misclassified samples suggesting the factor is associated with model mistakes. For example, an error ratio of 2x indicates a factor is 2x more likely to be selected among misclassified samples than overall. An error ratio less than zero indicates a factor is less likely to appear among misclassified samples suggesting the model is robust to the factor. Since some factors are selected only for a few images, we exclude factors selected for five or fewer images in our analysis. Doing so excludes style and brightness.

**Texture, occlusion, and darker lighting are most associated with model disparities across incomes and regions.** We examine the five factors most associated with model mistakes (measured using error ratio). Overall, we find mistakes for CLIP with a ViT-B/32 encoder are most associated with *texture, occlusion, or objects appearing too*

*small* as shown in Figure 9. For example, *texture* appears +0.88x more among CLIP’s mistakes than overall. Similarly, *occlusion* appears +0.76x and *smaller* +0.73x more so among mistakes. We conduct  $\chi^2$ -test to verify such differences in factor prevalence are statistically significant (see Appendix A.4).

We find these vulnerabilities also explain the performance disparities we observe for low incomes and regions with lower performance (Africa). In Figure 9 we show the five factors most associated with model mistakes across incomes (and across regions in Figure 10). We find in the low income bucket, *texture* has the largest error ratio with *texture* 1.7x more likely to be selected among misclassifications in the low income bucket. On the other hand, for the high income bucket misclassifications are associated with quite different factors. For example, *smaller* objects are most associated with mistakes in the high income bucket. We find a similar trend for across regions with *texture*, *occlusion*, and *darker* lighting most associated with mistakes in the region of Africa. We also detail model strengths by measuring factors that are much less likely to appear among mistakes in Appendix A.4. For example, we find CLIP is much less likely to misclassify images with *partial views* of objects.

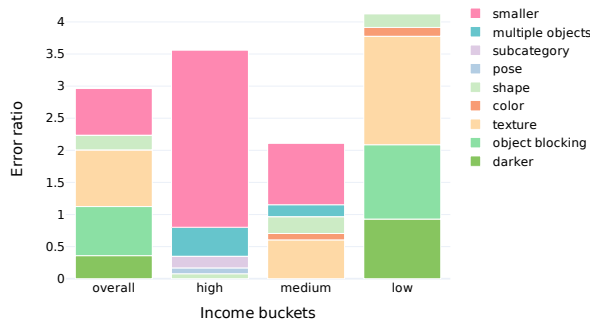


Figure 9: **CLIP is most vulnerable to texture, occlusion, and darker lighting for low incomes.** Figure shows the five factors most associated with model mistakes across incomes. The area within each bar represents the error ratio measuring how much more likely a factor is selected among the model’s misclassified samples.

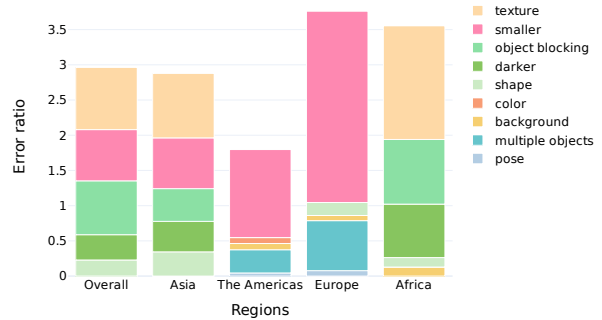


Figure 10: **CLIP is vulnerable to texture and occlusion in Africa and Asia.** The five factors most associated with model mistakes in each region. The area within each bar represents the error ratio measuring how much more likely a factor is selected among the model’s misclassified samples.

### 5.3.1 Some model vulnerabilities are class-specific

Beyond explaining performance disparities across regions or income buckets overall, our factor labels enable us to explain vulnerabilities for specific classes. We show in Table 2 the factors most associated with mistakes for classes with the lowest performance across regions. We find the lowest performance is for images in the region of Africa with each class exhibiting class-specific vulnerabilities. For *shaving*, *shape* is most associated with the low performance as it’s 5.8x more likely to appear among mistakes in Africa. For *sofas*, *texture* is 7.2x more likely to appear among mistakes. We find a similar pattern for classes with the low performance across incomes in Appendix A.4 and A.3. These strong shifts in error ratios point to class-specific vulnerabilities.

Next we study vulnerabilities across a range of model architectures and learning procedures.



Class	Region	Factors most associated with mistakes
shaving	Africa	shape (+5.8x), pattern (+0.2x), background (+0.1x)
sofas	Africa	texture (+7.2x), pattern (+0.3x), pose (+0.1x)
bathrooms	Africa	background (+1.1x), pose (+0.2x), color (+0.1x)
kitchen sinks	Africa	color (+0.6x), background (+0.2x), pose (+0.2x)
showers	Africa	background (+1.2x), pose (+0.4x), multiple objects (-1.0x)

Table 2: Class-specific vulnerabilities surfaced by our factor labels. We show vulnerabilities for the classes with lowest regional performance.

## 6 The effect of architecture and training procedure on mistake types

The factor labels also allow us to compare vulnerabilities across models. We first study vulnerabilities across a range of vision models then we show mitigating the most common vulnerability (to *texture*) can improve performance disparities across incomes and geographies.

### 6.1 Comparing vulnerabilities across architectures and training procedures

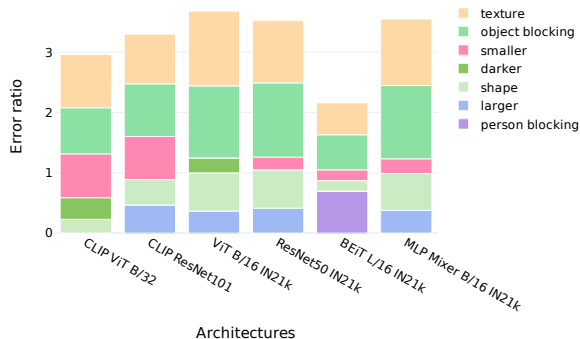


Figure 11: **Model vulnerabilities are similar across architectures and learning procedures.** Figure shows the five factors that are most associated with each model’s mistakes where the area of each bar indicates the error ratio.

In Figure 11, we examine model vulnerabilities across architectures and training methodologies. We find that, for all models, *texture*, *occlusion*, and *shape* are consis-

Top-5 Accuracy	Overall	<i>Images Marked with Texture</i>		
		low income	Africa	Asia
ResNet-50	32.2	25.2	18.6	24.4
Texture debiased	<b>33.0</b>	<b>29.3</b>	<b>21.6</b>	<b>25.0</b>

Table 3: Texture debiasing [10] can improve performance across low income buckets and regions with lower performance for images marked with texture as a distinctive factor.

tently among the factors most associated with model mistakes. While texture is known to be a bias specifically for convolutional-models [10, 15], we find regardless of architecture or training procedure models have similar vulnerabilities.

### 6.2 Improving performance disparities by mitigating texture bias

Our analysis in Section 5.3 reveals *texture* is most associated with model’s performance discrepancy across incomes and geographies. Can we improve this performance disparity by mitigating models’ reliance on texture? To assess this, we compare in Table 3 the performance of a standard ResNet-50 trained on ImageNet-1k compared to a ResNet-50 trained to mitigate texture bias [10]. Since these are trained on ImageNet-1k (1 million images) rather than ImageNet-21k (14 million images), the overall performance is lower than other models we studied earlier (see Appendix A.5). Controlling for pretraining data, we observe a boost of +0.8% in overall top-5 accuracy for the model mitigating texture bias. On the relevant subset of images (those marked with texture as a distinctive factor), we find consistent improvements in accuracy for the low income bucket +4.1% and in lower performing regions (Africa +3.0% and Asia +0.6%). This suggests that factor labels do not only explain model mistakes, but can also reveal potential mitigations to combat performance disparities.

## 7 Related work

Rojas et al. [23], Singh et al. [26], Goyal et al. [12, 14] have used Dollar Street to understand disparities in model performance between geographic and income groups, finding that many models perform better on images from Europe and the Americas, as well as those from higher household incomes. While many of the aforementioned works focus on how model architectures affect disparity findings, additional studies [7, 24] investigate the dataset itself to identify causes of variation in model performance, including the broader geographical distribution of images as compared to the model’s training data. A number of datasets [20, 8, 17] and dataset auditing tools [28] have since been developed with geographic diversity in mind. De Vries et al. [7] investigated the use of English as a “base language” for data collection. Empirical studies have shown that the “concreteness” of English words can vary greatly where crowd-sourced annotators consider words like “human” and “bobsled” more concrete than words like “recreation” and “outage” [6], and previous discussions of “class label perceptions” distinguish physical properties of a substance (such as orientation or texture) from a purpose relative to the specific being that interacts with the substance, such as being “sit-on-able” [11]. The relationship between the true meaning of a concept versus its perceptible form remains contested for both models [4] and humans [18]. Beyond Dollar Street, other works study variations in representations of concepts across visual factors including pose, background, occlusion, etc. within ImageNet [16] and collect supplementary multi-class labels [30, 5, 25]. Barbu et al. [3] created a benchmark to measure a model’s robustness to backgrounds, rotations, and viewpoints.

## 8 Conclusion

In this work, we take a step towards explaining why disparities in object-recognition systems arise. We annotate images from the Dollar Street dataset with distinguishing factors in order to explain how objects differ across incomes and geographies. Using these labels, we identify vulnerabilities in CLIP, a foundation model with impressive zero-shot classification performance. We find disparities in model performance are associated with texture, occlusion, and darker lighting. Finally, we surface initial

promising mitigations such as texture debiasing that can improve performance disparities. This shines light on a promising research direction leveraging techniques in robustness for fairness gains. In future work, we plan to explore further targeted mitigations can improve performance disparities in vision systems. While our conclusions are limited by the number of samples and representative diversity of the Dollar Street dataset, we hope by releasing our factor annotations we spur further research into equitable vision systems. We have released the DollarStreet factor annotations at [https://github.com/facebookresearch/dollarstreet\\_factors](https://github.com/facebookresearch/dollarstreet_factors).

**Acknowledgements** We would like to acknowledge *Adina Williams, Sahir Gomez, Somya Jain, Quentin Duval, Ida Cheng, Austin Miller* for their helpful discussions, support, and insightful feedback.

## References

- [1] Detailed income calculations for dollar street. <https://drive.google.com/file/d/0B0HB08a-a9MbZfJZMTFEUkx0RWc/view?resourcekey=0-XFuTX8d2FyhmrDhMp35LDA>. Accessed: 2023-01-24. 3
- [2] Hangbo Bao, Li Dong, Songhao Piao, and Furu Wei. Beit: Bert pre-training of image transformers. In *International Conference on Learning Representations*, 2021. 6
- [3] Andrei Barbu, David Mayo, Julian Alverio, William Luo, Christopher Wang, Dan Gutfreund, Josh Tenenbaum, and Boris Katz. Objectnet: A large-scale bias-controlled dataset for pushing the limits of object recognition models. In H. Wallach, H. Larochelle, A. Beygelzimer, F. d’Alché-Buc, E. Fox, and R. Garnett, editors, *Advances in Neural Information Processing Systems*, volume 32. Curran Associates, Inc., 2019. URL <https://proceedings.neurips.cc/paper/2019/file/97af07a14cacba681feacf3012730892-Paper.pdf>. 10

- [4] Emily M. Bender and Alexander Koller. Climbing towards NLU: On meaning, form, and understanding in the age of data. In *Proceedings of the 58th Annual Meeting of the Association for Computational Linguistics*, pages 5185–5198, Online, July 2020. Association for Computational Linguistics. doi: 10.18653/v1/2020.acl-main.463. URL <https://aclanthology.org/2020.acl-main.463>. 10
- [5] Lucas Beyer, Olivier J. Hénaff, Alexander Kolesnikov, Xiaohua Zhai, and Aäron van den Oord. Are we done with imagenet? *CoRR*, abs/2006.07159, 2020. URL <https://arxiv.org/abs/2006.07159>. 10
- [6] Marc Brysbaert, Amy Beth Warriner, and Victor Kuperman. Concreteness ratings for 40 thousand generally known english word lemmas. *Behavior research methods*, 46(3):904–911, 2014. 10
- [7] Terrance De Vries, Ishan Misra, Changhan Wang, and Laurens Van der Maaten. Does object recognition work for everyone? In *Proceedings of the IEEE/CVF Conference on Computer Vision and Pattern Recognition Workshops*, pages 52–59, 2019. 1, 2, 10
- [8] Abhimanyu Dubey, Vignesh Ramanathan, Alex Pentland, and Dhruv Mahajan. Adaptive methods for real-world domain generalization. In *Proceedings of the IEEE/CVF Conference on Computer Vision and Pattern Recognition*, pages 14340–14349, 2021. 10
- [9] Dominik Endres and Johannes Schindelin. A new metric for probability distributions. *Information Theory, IEEE Transactions on*, 49:1858 – 1860, 08 2003. doi: 10.1109/TIT.2003.813506. 4
- [10] Robert Geirhos, Patricia Rubisch, Claudio Michaelis, Matthias Bethge, Felix A. Wichmann, and Wieland Brendel. ImageNet-trained CNNs are biased towards texture; increasing shape bias improves accuracy and robustness. URL <http://arxiv.org/abs/1811.12231>. 9, 22
- [11] James J. Gibson. *The Ecological Approach to Visual Perception: Classic Edition*. Houghton Mifflin, 1979. 10
- [12] Priya Goyal, Quentin Duval, Isaac Seessel, Mathilde Caron, Ishan Misra, Levent Sagun, Armand Joulin, and Piotr Bojanowski. Vision models are more robust and fair when pretrained on uncurated images without supervision. URL <http://arxiv.org/abs/2202.08360>. 2, 10
- [13] Priya Goyal, Mathilde Caron, Benjamin Lefaudeux, Min Xu, Pengchao Wang, Vivek Pai, Mannat Singh, Vitaliy Liptchinsky, Ishan Misra, Armand Joulin, et al. Self-supervised pretraining of visual features in the wild. *arXiv preprint arXiv:2103.01988*, 2021. 6
- [14] Priya Goyal, Adriana Romero Soriano, Caner Hazirbas, Levent Sagun, and Nicolas Usunier. Fairness indicators for systematic assessments of visual feature extractors. In *2022 ACM Conference on Fairness, Accountability, and Transparency*, 2022. doi: 10.1145/3531146.3533074. URL <https://doi.org/10.1145/3531146.3533074>. 1, 3, 5, 10, 13, 18, 22
- [15] Katherine Hermann, Ting Chen, and Simon Kornblith. The origins and prevalence of texture bias in convolutional neural networks. *Advances in Neural Information Processing Systems*, 33:19000–19015, 2020. 9
- [16] Badr Youbi Idrissi, Diane Bouchacourt, Randall Balestriero, Ivan Evtimov, Caner Hazirbas, Nicolas Ballas, Pascal Vincent, Michal Drozdal, David Lopez-Paz, and Mark Ibrahim. Imagenet-x: Understanding model mistakes with factor of variation annotations. *arXiv preprint arXiv:2211.01866*, 2022. 3, 7, 10
- [17] Zu Kim, André Araujo, Bingyi Cao, Cam Askew, Jack Sim, Mike Green, N Yilla, and Tobias Weyand. Towards a fairer landmark recognition dataset. *arXiv preprint arXiv:2108.08874*, 2021. 10
- [18] Ben Phillips. The shifting border between perception and cognition. *Noûs*, 53, 06 2019. doi: 10.1111/nous.12218. 10
- [19] Alec Radford, Jong Wook Kim, Chris Hallacy, Aditya Ramesh, Gabriel Goh, Sandhini Agarwal, Girish Sastry, Amanda Askell, Pamela Mishkin, Jack

- Clark, Gretchen Krueger, and Ilya Sutskever. Learning transferable visual models from natural language supervision. URL <https://arxiv.org/abs/2103.00020v1>. 2, 5
- [20] Vikram V Ramaswamy, Sing Yu Lin, Dora Zhao, Aaron B Adcock, Laurens van der Maaten, Deepti Ghadiyaram, and Olga Russakovsky. Beyond web-scraping: Crowd-sourcing a geographically diverse image dataset. *arXiv preprint arXiv:2301.02560*, 2023. 10
- [21] Tal Ridnik, Emanuel Ben-Baruch, Asaf Noy, and Lihi Zelnik-Manor. Imagenet-21k pretraining for the masses. In *Thirty-fifth Conference on Neural Information Processing Systems Datasets and Benchmarks Track (Round 1)*, 2021. 3, 6, 13, 18
- [22] Michael Roberts, Derek Driggs, Matthew Thorpe, Julian Gilbey, Michael Yeung, Stephan Ursprung, Angelica I Aviles-Rivero, Christian Etmann, Cathal McCague, Lucian Beer, et al. Common pitfalls and recommendations for using machine learning to detect and prognosticate for covid-19 using chest radiographs and ct scans. *Nature Machine Intelligence*, 3(3):199–217, 2021. 1
- [23] William A Gaviria Rojas, Sudnya Diamos, Keertan Ranjan Kini, David Kanter, Vijay Janapa Reddi, and Cody Coleman. The dollar street dataset: Images representing the geographic and socioeconomic diversity of the world. In *Thirty-sixth Conference on Neural Information Processing Systems Datasets and Benchmarks Track*, 2022. URL <https://openreview.net/forum?id=qnfYsave0U4>. 1, 2, 6, 10, 22
- [24] Shreya Shankar, Yoni Halpern, Eric Breck, James Atwood, Jimbo Wilson, and D Sculley. No classification without representation: Assessing geodiversity issues in open data sets for the developing world. *arXiv preprint arXiv:1711.08536*, 2017. 10
- [25] Vaishaal Shankar, Rebecca Roelofs, Horia Mania, Alex Fang, Benjamin Recht, and Ludwig Schmidt. Evaluating machine accuracy on ImageNet. In Hal Daumé III and Aarti Singh, editors, *Proceedings of the 37th International Conference on Machine Learning*, volume 119 of *Proceedings of Machine Learning Research*, pages 8634–8644. PMLR, 13–18 Jul 2020. URL <https://proceedings.mlr.press/v119/shankar20c.html>. 10
- [26] Mannat Singh, Laura Gustafson, Aaron Adcock, Vinicius de Freitas Reis, Bugra Gedik, Raj Prateek Kosaraju, Dhruv Mahajan, Ross Girshick, Piotr Dollár, and Laurens van der Maaten. Revisiting weakly supervised pre-training of visual perception models. In *Proceedings of the IEEE/CVF Conference on Computer Vision and Pattern Recognition (CVPR)*, pages 804–814, June 2022. 10
- [27] Ilya O Tolstikhin, Neil Houlsby, Alexander Kolesnikov, Lucas Beyer, Xiaohua Zhai, Thomas Unterthiner, Jessica Yung, Andreas Steiner, Daniel Keysers, Jakob Uszkoreit, et al. Mlp-mixer: An all-mlp architecture for vision. *Advances in Neural Information Processing Systems*, 34:24261–24272, 2021. 6
- [28] Angelina Wang, Alexander Liu, Ryan Zhang, Anat Kleiman, Leslie Kim, Dora Zhao, Iroha Shirai, Arvind Narayanan, and Olga Russakovsky. Revise: A tool for measuring and mitigating bias in visual datasets. *International Journal of Computer Vision*, pages 1–21, 2022. 10
- [29] Xiang Xu, Wan-Quan Liu, and Ling Li. Low resolution face recognition in surveillance systems. *Journal of Computer and Communications*, 2:70–77, 2014. 6
- [30] Sangdoon Yun, Seong Joon Oh, Byeongho Heo, Dongyoon Han, Junsuk Choe, and Sanghyuk Chun. Re-labeling imagenet: from single to multi-labels, from global to localized labels. *CoRR*, abs/2101.05022, 2021. URL <https://arxiv.org/abs/2101.05022>. 10

## A Appendix

### A.1 Annotating Dollar Street with factor labels

#### A.1.1 DollarStreet Statistics

Region	Income Level		
	low	medium	high
Africa	2141	1443	280
Asia	1362	8673	1424
Europe	0	1443	1455
The Americas	339	2093	1223

Table 4: Number of images for each region, income level pair in Dollar Street.

Table 4 shows the number of images in Dollar Street for each income and region pairing. We observe the distribution across images and regions is far from uniform, implying region and income distributions skew of counts are entangled. Consequently, we present both region and income comparisons where appropriate in our analysis.


#### A.1.2 Prototypical Image Selection

We define prototypical images for each class as those correctly classified by ResNet-50 model with the highest confidence. We use a ResNet-50 model pre-trained on ImageNet21k from Ridnik et al. [21]. We select the ImageNet classes that overlap with Dollar Street labels, using the mapping as defined in [14]. We use a soft-max over the sub-section of ImageNet classes that are in the mapping. We take the top predictions and confidence for these ImageNet classes and use the defined mapping from IN21k to Dollar Street in order to make DollarStreet class predictions. Out of the box, the model does not perform well on DollarStreet. Running a full pass over the dataset with Batch Norm in train mode, without any updates to the model weights, helps with the distribution shift from ImageNet to DollarStreet images, meaning overall accuracy is higher.


We select the three images that the model predicts successfully with the highest confidence. If such images do not exist, prototypical images are hand-selected. Table 5 shows the prototypical images used for five classes.

#### A.1.3 Annotation Setup

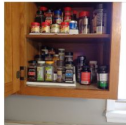
Figure 12 shows an example of the annotation task. Annotators select the factors distinguishing each image among sixteen factors such as pose, various forms of occlusion, size, style, type or breed. Annotators can select any number of distinctive factors for each image. We source 10 annotators through a third party vendor from South East Asia. In addition, we ask annotators to provide text descriptions to account for factors outside the sixteen we provide. We trained annotators with examples so that they were familiar with the task before annotating the target images. We had intermediate QA from the third party vendor monitoring annotations for quality. We also ask annotators whether they agree with the original class label for each image.




left1



left2



left3



spices

1. Can I rate this job?

Yes, I can rate this job

No, I cannot rate this job (content doesn't load, contains PII)

2. Select (all) categories that make the RIGHT image different from the group of LEFT images

Pose of Subject

Subject's Location/Placement

Object is partially present (eg: cropped out)

Object partially blocked by another object

Object partially blocked by a person

Another Object is present

Object is small relative to the image frame

Object is large relative to the image frame

Lighting is Brighter

Lighting is Darker

Background

Color

Shape

Texture

Pattern

Media style

Subcategory

Describe more about your selections in question 2

Describe in 1-word what the primary difference is between the left images and right image?

[RIGHT IMAGE] Do you agree with the label(s) for the RIGHT image?

Yes

No

[RIGHT IMAGE] If you disagree with the labels for the RIGHT image, please explain in 1-2 sentences why you disagree

Figure 12: Example annotation task.

Class	Prototypical Images		
grains			
plates			
power outlets			
cleaning floors			
toothbrushes			

Table 5: Prototypical images used for five classes.

#### A.1.4 Label Agreement Annotation Setup

Country	Number of annotators
India	8
Nigeria	9
Brazil	13
United Arab Emirates	6
United States	8

Table 6: Annotator breakdown for label agreement task.

For our follow up annotations about label agreement, we sourced 44 annotators from 5 different countries, with the full demographics shown in Table A.1.4. We asked one annotator per country about each image in question. In Table 13, we show example images from the three most disputed classes, along with alternative labels suggested by annotators. In Table 7, we show the classes with the highest and lowest levels of disagreement among annotators.

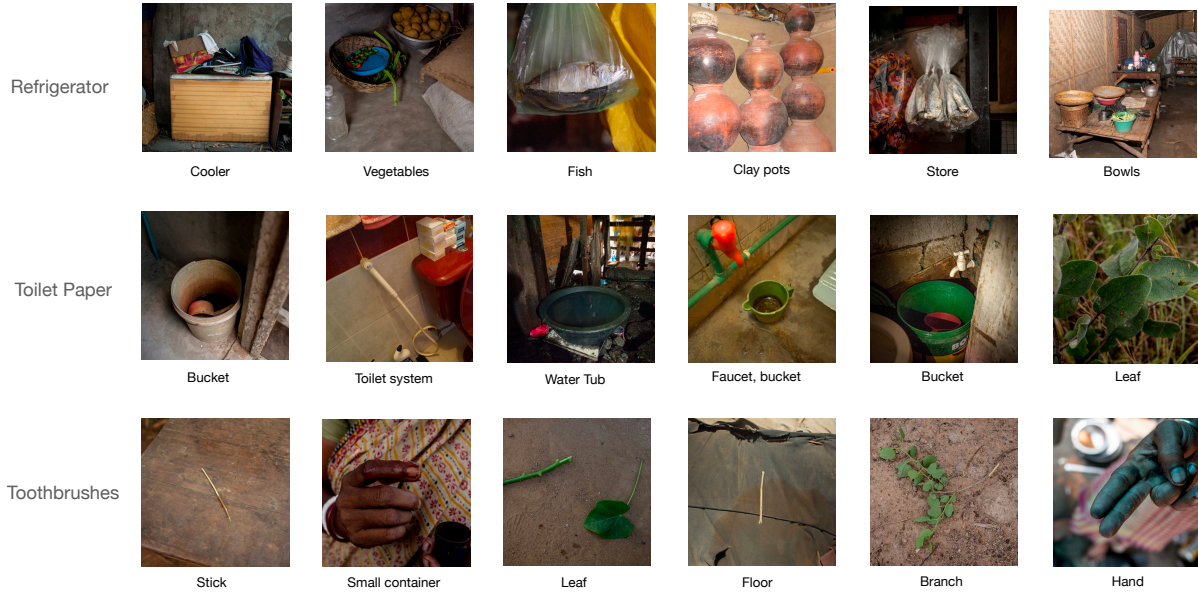


Figure 13: Randomly sampled example images and alternative labels given for the three classes with most disagreement. The original class label is shown on the left, and the alternative label given by the annotator shown below each image.

class	% disagreement	class	% disagreement
toilet paper	88.4	medication	10.0
refrigerators	83.5	fruit trees	11.8
toothbrushes	79.3	plates of food	12.3
sofas	77.8	trash	14.3
diapers	72.0	cleaning floors	14.5
armchairs	70.6	ceilings	15.0
showers	66.3	homes	15.0
kitchen sinks	64.5	books	15.0
wall clocks	63.2	cooking pots	19.8
radios	60.4	wheel barrows	20.0

Table 7: Top ten classes with the highest percentage of annotators who *disagreed* (left) and *agreed* (right) with the original class label



## A.2 How do objects vary across incomes and geographies?

We show the most dissimilar classes across incomes and regions by comparing the Jensen-Shannon Distance of the factor annotation distributions in Tables 8 and 9.

class	income bucket	differentiating factors
roofs	low vs. high	subcategory, pose, smaller
ceilings	low vs. high	pose, subcategory, texture
diapers	low vs. high	color, shape, texture
radios	low vs. high	color, shape, subcategory
floors	low vs. high	texture, pose, pattern
sofas	low vs. high	color, texture, multiple objects
kitchen sinks	low vs. high	shape, pose, background
toilet paper	low vs. high	color, pose, background
wardrobes	low vs. high	background, pattern, color
mosquito protections	low vs. high	color, subcategory, pattern

Table 8: Classes with most stark differences in factor distributions by Jensen-Shannon Distance (JSD) across incomes.

class	regions	distinctive factors
chickens	Asia vs. Europe	partial view, color, shape
chickens	Europe vs. Africa	pose, partial view, color
diapers	The Americas vs. Africa	pose, color, partial view
pet foods	Asia vs. The Americas	color, texture, pattern
pet foods	Asia vs. Europe	pattern, subcategory, color
ceilings	Europe vs. Africa	pose, subcategory, texture
roofs	Europe vs. Africa	subcategory, pose, texture
car keys	Asia vs. Europe	pattern, partial view, subcategory
make up	Europe vs. Africa	background, subcategory, pattern
goats	Asia vs. Africa	pattern, color, subcategory

Table 9: Classes with most stark differences in factor distributions by Jensen-Shannon Distance (JSD) across regions

We show the most similar classes across incomes and regions using the same procedure of comparing Jensen-Shannon Distance of the factor annotation distributions in Tables 10 and 11.

class	income buckets	distinctive factors
vegetable plots	low vs. high	multiple objects, background, color
phones	medium vs. high	background, pose, multiple objects
pens	medium vs. high	color, background, pattern
bikes	low vs. high	background, subcategory, smaller
armchairs	medium vs. high	color, background, pose
latest furniture bought	medium vs. high	subcategory, background, color
child rooms	medium vs. high	pose, pattern, color
wall clocks	medium vs. high	color, pose, shape
cooking utensils	medium vs. high	pose, shape, pattern

Table 10: Classes most similar in factor distributions by Jensen Shannon Distance across incomes

class	regions	distinctive factors
vegetable plots	The Americas vs. Africa	pose, background, pattern
phones	Asia vs. Europe	pose, background, color
pens	Europe vs. Africa	pose, color, pattern
wheel barrows	Europe vs. The Americas	color, pose, background
ceilings	Asia vs. Africa	subcategory, pattern, texture
pets	Asia vs. Europe	background, pattern, subcategory
stoves	Asia vs. Africa	subcategory, color, pattern
menstruation pads	Asia vs. The Americas	pose, subcategory, pattern
tv's	Europe vs. The Americas	partial view, subcategory, background
everyday shoes	Europe vs. The Americas	color, partial view, shape

Table 11: Classes most similar in factor distributions by Jensen Shannon Distance (JSD) across regions

### A.3 Evaluation Setup

**CLIP Prompt Engineering** We use CLIP in a zero shot setting, where we prompt the model using the set of Dollar Street classes (e.g. *medication, plates of food*) for each image to generate predictions. We generate the text prompts for CLIP by combining the 80 prompt templates used in the original CLIP paper with each Dollar Street class name, substituting `_` for spaces. We consider an image correctly predicted if the top 5 classes predicted by CLIP is associated with the photo. *Note: Most photos in DollarStreet have only one label, but a small subset of (638) images containing multiple class labels (e.g. (cups, plates, dish racks) and (child rooms, kids bed, beds)).*

**ImageNet21k as a shared taxonomy** For models outside of CLIP, we use ImageNet21k to ground our models in a shared taxonomy. Following Goyal et al. [14], we map the ImageNet21k labels to DollarStreet classes. We consider the image correctly classified if any of the top 5 ImageNet21k classes predicted by the model are mapped to any of the DollarStreet classes associated with the photo. We note that the mapping is not 1:1, and multiple classes in DollarStreet have multiple classes in ImageNet 21k that map to the single class. All of the models used for evaluation excluding CLIP and SEER are trained on ImageNet 21k. SEER is pre-trained in a self-supervised manner, and the model is fine-tuned on the 108 classes in ImageNet 21k that overlap with DollarStreet prior to evaluation. For ImageNet-21k pretraining, we use models from Ridnik et al. [21].

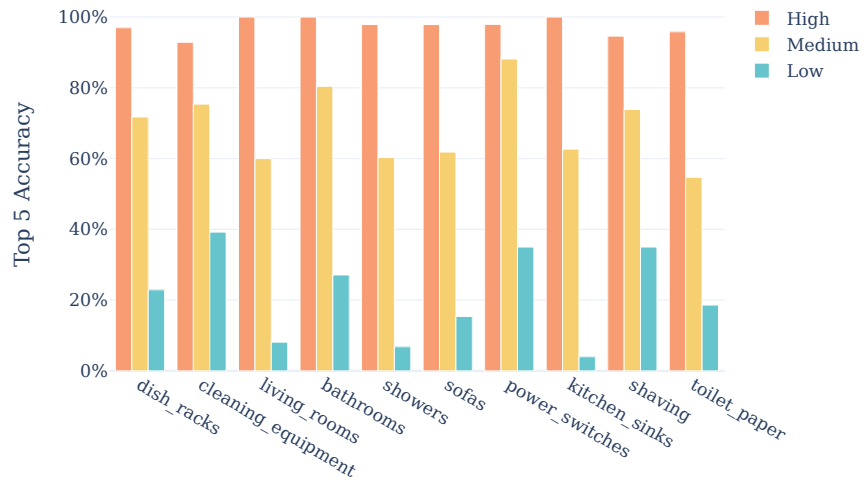
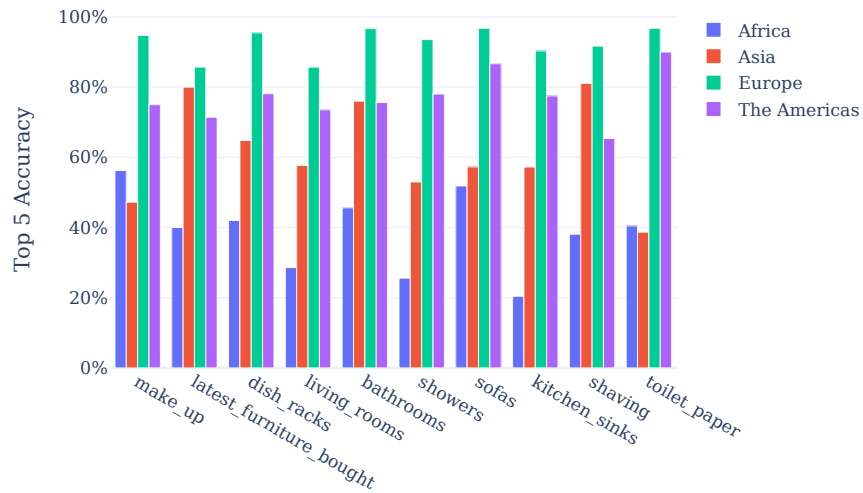


Figure 14: 10 classes with biggest performance discrepancy over regions (top) and income bucket (bottom).

**Class level performance disparities** Figure 14 and show the top 10 classes with the biggest performance disparity between groups for regions and incomes. We define the largest performance discrepancy as the maximum difference in accuracy between any two regions (or income buckets). At a class level, we find that the discrepancy in accuracy can be

stark - over 50% for the classes with the widest gap. For both incomes and geographies, we find that the differences mostly pertain to items in kitchens (*dish racks, kitchen sinks*) and items in bathrooms (*showers, shaving, toilet paper, bathrooms*).

#### A.4 Explaining model performance disparities with factor labels

As part of our analysis of model performance disparities, we investigate the impact of pretraining class balance and image quality. In Table 12, we show the Pearson correlation coefficients and p-values between each model’s top-5 accuracy and the Image DPI, a measure of image resolution. In Table 13, we show the Pearson correlation coefficients and p-values between each model’s top-5 accuracy and the ImageNet-21K class count. We excluded CLIP from this analysis as CLIP was trained on a proprietary dataset.

Model	Correlation Between Top 5 Accuracy and Image DPI
ViT	-0.019 (p = 0.035)
ResNet50	-0.023 (p = 0.008)
MLPMixer	-0.026 (p = 0.002)
BeIT	-0.003 (p = 0.72)
SEER	-0.016 (p = 0.057)
CLIP	-0.035 (p = 0.00005)

Table 12: Pearson Correlation coefficients and p-values between each model’s top-5 accuracy and image quality, as measured by DPI.

Model	Correlation Between Top-5 Accuracy and Class Count
ViT	0.126 (p < 0.0001)
ResNet50	0.142 (p < 0.0001)
MLPMixer	0.135 (p < 0.0001)
BeIT	0.222 (p < 0.0001)
SEER	0.103 (p < 0.0001)

Table 13: Pearson Correlation coefficients and p-values between each model’s top-5 accuracy and ImageNet-21K class counts. CLIP is not included, as it was trained on a proprietary dataset.

Factors most associated with misclassifications differ considerably across regions and incomes. We find for the high income bucket, objects marked as *smaller* are most associated with mistakes, appearing +2.8x more among mistakes. On the other hand, *texture* which is not among the top five factors among mistakes in the high income bucket is associated with mistakes in the medium and low income buckets. *Texture* is +0.6x and +1.7x more likely to appear among mistakes in the medium and low income buckets respectively. We also find in the low income bucket, factors such as *occlusion* and *darker lighting* to be associated with model mistakes, appearing +1.2x and +0.9x more so among mistakes in the low income bucket. This suggests specific factors such as *texture, occlusion, and darker lighting* are associated with the disparity in performance we observe across incomes.



Figure 15: Shows the full error ratios for each factor per income bucket (top) and region (bottom). An error ratio higher than zero indicates the factor is more associated with model mistakes; less than zero indicates the factor is less likely to appear among a model’s mistakes.

**Factors associated with mistakes differ across regions.** We also measure the factors associated with model mistakes across regions in Figure 10. In Asia we observe the factors most associated with mistakes are similar to those associated

with mistakes overall. However, we find distinctive factors are associated with mistakes across each of the other regions. In the Americas, we find *smaller objects* (+1.2x more likely to appear among mistakes), followed by images with *multiple objects* (+0.3x). Similarly in Europe, *smaller objects* and *multiple objects* are most associated with mistakes appearing +2.8x and +0.7x more so among mistakes respectively. In Africa however, we find instead *texture* (+1.6x) most associated with mistakes, followed by *occlusion* (+0.9x) and *darker lighting* (+0.8x). This suggests the disparity due to lower performance in regions such as Africa are associated with distinct factors related to *texture*, *occlusion*, and *darker lighting*.

**Statistical significance of error ratios for top factors.** To confirm the top factors associated with model mistakes measured by our error ratio are statistically significant. We conduct a Chi-Squared test comparing the overall distribution of counts of the top factors to their distribution of counts among misclassifications. We find a statistically significant difference with a Chi-Squared statistic of 21.7 (p-value =0.0002).

**Factors most associated with largest discrepancies for classes across income buckets.** We show the three factors most associated with model mistakes for the classes across income buckets with largest performance gap in Table A.4. Trends are similar to those shown in the main paper for the largest disparity per region.

Class	Income	Factors associated with mistakes
sofas	low	pattern (+0.5x), background (+0.3x), pose (+0.2x)
toilet paper	low	texture (+3.3x), shape (+2.7x), color (+0.8x)
living rooms	low	background (+0.8x), pose (+0.0x), color (-0.1x)
kitchen sinks	low	color (+0.5x), background (+0.3x), pose (+0.2x)
showers	low	background (+0.9x), pose (+0.3x), pattern (-0.5x)

Table 14: Class-specific vulnerabilities surfaced by our factor labels. We show vulnerabilities for the classes with lowest income performance. The values in parenthesis indicate how much more likely a factor is to appear for misclassified samples.

## A.5 The effect of architecture and training procedure

**Texture debiasing experimental details** To measure the effect of reducing texture bias from Geirhos et al. [10], we create a mapping from Dollar Street classes to ImageNet-1k similar to Rojas et al. [23]. We initialize the mapping by matching the embedding similarity of each class name to its nearest neighbors from ImageNet-1k using a pre-trained Spacy language model `eng-large` <https://spacy.io/usage/linguistic-features#vectors-similarity>. We then manually correct any issues in this mapping to produce ImageNet-1k mappings for approximately half of the Dollar Street classes. Note for all other analysis we use the ImageNet-21k mapping from Goyal et al. [14].

**Additional experiment: choice of encoder architecture can also improve performance discrepancy** We found CLIP with a ViT encoder has a smaller error ratio for objects marked as *larger* compared to CLIP with a ResNet-101 encoder in Figure 11. Does this insight imply improved performance robustness to objects associated with the larger factor? If so, we expect images annotated with the larger factor to show improved performance for the ViT encoder. We compare the top-5 accuracy of the ViT versus ResNet encoder for images marked with larger factor. This suggests modeling choices such as architecture are potential mitigations to improve robustness to certain factors. We find ViT

classification accuracy is 80.4% compared to ResNet encoder’s 73.9% suggesting the improved factor error ratio of the ViT encoder to larger objects yields a gain in performance. For images marked as *larger*, can such a performance improvement also improve the disparity we observe across incomes? Although the number of samples is limited ( $\sim 50$  images), we find ViT’s improved robustness to larger objects decreases the gap between low and high income buckets for those images by 15% compared to the ResNet encoder. This not only suggests choices such as architecture can influence the model disparities we observe, but that the factor annotations can help uncover mitigations to certain factors associated mistakes to improve the disparities in performance across incomes and geographies. This preliminary finding offers an encouraging direction to improve the model disparities we observe through the labeled factors.

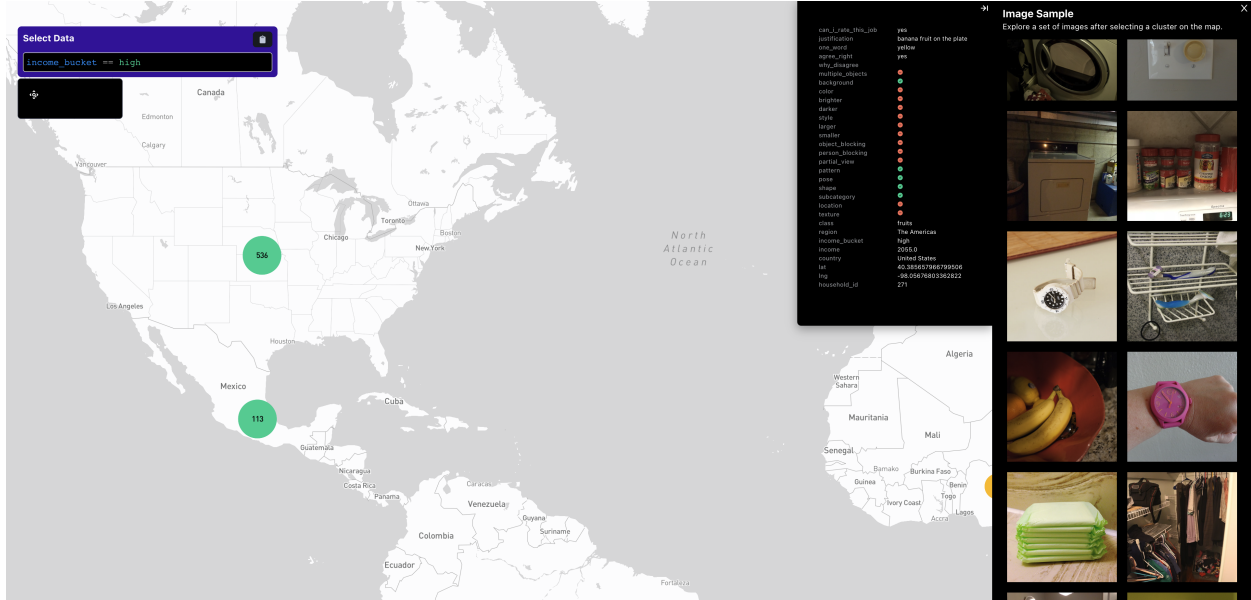
## A.6 Interactive factor dashboard

We show screenshots of our interactive dashboard for exploring the factor labels across regions in Figures 16 and 17. The dashboard allows for interactive queries by region, income, factor label. Each query yields sample images, which you can interactively explore annotations for as shown in 17. We hope this tool will allow researchers to easily explore factor labels associated with images across axes such as regions or incomes to spur further research into reliable vision systems.

Figure 16: Interactive dashboard for Dollar Street factor annotations with an income and factor label query (for texture).



Figure 17: Interactive dashboard for Dollar Street factor annotations illustrating an example of the annotations.



## A.7 Sample images

Country	Sample Images			
The Americas				
Africa				

Table 15: Examples of diaper images. Our factors surfaced that images of diapers in Dollar Street between regions differed most among *pose*, *color*, *partial view*.





Country				
Asia				
Africa				

Table 16: Examples of goat images. Our factors surfaced that images of goats in Dollar Street between regions differed most among *pattern, color, subcategory*

In Figures 16 and A.7 we show example images from classes and regions that were found to have some the starkest difference in factors, as measured by JSD.